Production of D-mesons in p+p and p+Pb collisions at LHC energies

R.C.Baral[1,*], S.K.Tripathy[1,2], M.Younus[1], Z. Naik[2], and P.K.Sahu[1]

[1]Institute of Physics, Bhubaneswar-751005, India
[2]Sambalpur University, Burla-768019, India

arXiv:1606.07971v2 [hep-ph] 24 Oct 2016

Abstract

We present theoretical model comparison with published ALICE results for D-mesons (D^0, D^+ and D^{*+}) in p+p collisions at $\sqrt{s}$ = 7 TeV and p+Pb collisions at $\sqrt{s_{NN}}$ = 5.02 TeV. Event generator HIJING, transport calculation of AMPT and calculations from NLO(MNR) and FONLL have been used for this study. We found that HIJING and AMPT model predictions are matching with published D-meson cross-sections in p+p collisions, while both under-predict the same in p+Pb collisions. Attempts were made to explain the R_{pPb} data using NLO-pQCD(MNR), FONLL and other above mentioned models.

1 Introduction

Relativistic heavy ion collisions at the RHIC [1] and the LHC [2] have given rise to a new phase of matter. When two heavy ions collide, a system of de-confined gluons and quarks within a very small volume is created. The initial energy density within this volume is found to be much larger than nuclear ground state energy density. This state of matter as we know today is called Quark Gluon Plasma (QGP) [3, 4]. The study of QGP is particularly important as it aims to produce a condition, which resembles the period when universe was only a few microseconds old. However, since this exotic system created in the experiments exists only for a very short period of time and is not directly observable, only signals originating from the matter itself that survive and are measured after the collisions can provide a window into the nature of the QGP [5, 6]. With high statistics data already accumulated at the Large Hadron Collider at CERN, the scientific community has an enormous task to analyse, and explain these observations and extract information about the properties of the QGP. These analyses are also leading the way for additional measurements and will become available for studies with all the major experiments, like STAR [7, 8], ALICE [9, 10] and proposed CBM at FAIR [11, 12].

One of the prominent signatures coming out of the QGP phase is jet quenching [13]. High momentum hadron spectra are observed to be highly suppressed relative to those in p+p collisions [14,15], suggesting a quenching effect due to deconfined matter. A similar effect is observed for high p_T charm or beauty quarks with most recent results showing suppression of D or B mesons to same order as that of light partons [16, 17]. However before going into hot and dense matter effects, it is absolute necessary to fix the baseline for such observations. In heavy ion scenario, p+p collisions serve as the baseline for such observations, assuming that no nuclear effects are present when p+p is scaled to p+Pb or Pb+Pb data only by a factor. On the other hand, it has been suggested that the modification in spectra of the observed particles in the heavy ion collision have effects of cold nuclear matter [18] before formation of QGP which are often masked by hot and dense matter effects. So it is important to discern the contributions of

*ramachandrabaral@yahoo.co.in

the cold nuclear effects from all other effects due to QGP on the final particle spectra. p+Pb collisions give us a unique opportunity to study these initial nuclear effects. The so called effect due to shadowing has been playing a role in the particle production scenario for a very long time. With the assumption that any nucleus is not just any conglomeration of protons is the very essence of this phenomenon. With LHC achieving its top collider energy, it may not be possible to overlook the shadowing features affecting the high gluon density within the nucleus. This phenomenon is also represented mathematically as shadowing ratio, $R_s \equiv F_A(x, Q^2)/(A^*F_p(x, Q^2))$, and has been found to deviate from unity as explained in early literatures [19], which makes this phenomenon as one of the most prominent feature of cold nuclear effects. On the other hand, another phenomenon that may affect the final particle spectra is multiple re-scattering of the colliding nucleons or their partons. This effect is known as Cronin effect [20]. This particular feature had been observed in the RHIC energy for non-photonic electrons' nuclear modification data, which shows an enhancement in the charm spectrum below $p_T < 4.0$ GeV [21]. The results suggest that this particular effect may be observed in the low and mid-p_T regions and may not be much effective in higher side of the momentum. We will come back to these two points later in our work.

Now let us move over to heavy quarks. A heavy quark owing to its large mass is produced much before the formation of quark gluon plasma [22]. It is also believed that heavy quarks remain free to probe thermalized medium without carrying any prior effects due to nucleus. From the recent result of p+Pb data and earlier d+Au data [23] on particle production, the value of R_{pPb} deviates from unity by almost 15% mostly in low and mid-p_T regions, which shows a considerable cold nuclear matter effect on heavy quark production [24]. The current work aims to highlight some of these initial nuclear effects on measured heavy meson spectra.

This paper is organised as follows. In the section 2 we discuss the various models employed for studying D-meson cross-section in p+p and p+Pb collisions at $\sqrt{s} = 7$ TeV and $\sqrt{s_{NN}} = 5.02$ TeV, respectively. In the section 3 we discuss our results with these models. Then we summarise our work in section 4.

2 Models used

2.1 The HIJING model

HIJING (Heavy-Ion Jet INteraction Generator) [25] is a Monte Carlo model designed mainly to explore the range of possible initial conditions that may occur in nuclear collisions at collider energies and to produce output that can be compared directly with a wide variety of nuclear collider experimental observables. The main features included in HIJING are as follows.
The formulation of HIJING is guided by Lund FRITIOF [26] and Dual Parton Model [27] for soft nuclear reaction at intermediate energy ($\sqrt{s_{NN}} \leq 20$ GeV). Multiple low p_T exchanges among the end point constituents are included to model initial state interactions. The PYTHIA [28] guides the pQCD processes where multiple minijet production with initial and final state radiation are involved. To reproduce p+A or A+A results, the Eikonal formalism is used to calculate the number of minijets per inelastic p+p collision. The model uses three-parameter Woods-Saxon nuclear density determined by electron scattering data [29]. A diffuse nuclear geometry decides the impact parameter dependence of the number of binary collisions [30].

The cross section for charm production formalism at the leading order is written as [31]

$$\frac{d\sigma_{cc}^{pp}}{dp_T^2 dy_1 dy_2} = K \sum_{a,b} x_1 f_a(x_1, p_T^2)\ x_2 f_b(x_2, p_T^2) \times \frac{d\hat{\sigma}_{ab}}{d\hat{t}}, \tag{1}$$

here a, b are the parton species, y_1, y_2 are the rapidities of the scattered partons, and x_1, x_2 are the fraction of momentum carried by the initial partons. A factor K, of value 2.0 has been used to account roughly for the higher order corrections. In HIJING, the parton structure functions,

$f_a(x_1, p_T^2)$ are the Duke-Owens [32] structure function set 1 and this is also implemented in PYTHIA. For the nuclear effect in A+A and p+A collisions, model follows the A dependence of the shadowing proposed in Ref. 33, 34 and uses its parameterization as

$$R_A(x) \equiv \frac{f_{a/A}(x)}{A\ f_{a/N}(x)} = 1 + 1.19\ \ln^{1/6}A[x^3 - 1.5(x_0 + x_L)x^2 + 3x_0x_Lx] - \left[\alpha_A(r) - \frac{1.08(A^{1/3} - 1)}{\ln(A+1)}\sqrt{x}\right]e^{-x^2/x_0^2}\ , \tag{2}$$

and $\alpha_A(r) = 0.1(A^{1/3} - 1)\frac{4}{3}\sqrt{1 - r^2/R_A^2}$.
Here r is the transverse distance of the interacting nucleon from its nucleus centre and R_A is the radius of the nucleus, and $x_0 = 0.1$ and $x_L = 0.7$. The most important nuclear dependence term is proportional to $\alpha_A(r)$ in Eq.2, which determines the shadowing for $x < x_0$, and the rest gives the overall very slow A dependence nuclear effect on the structure function for $x > x_L$.

We have used HIJING version 1.41.

2.2 The AMPT model

A Multiphase Transport Model (AMPT) [35] is a hybrid transport model, which was developed to address non-equilibrium many body dynamics. Initially it was designed to describe physics of p+A and A+A collisions for centre of mass energy from 5 GeV to 5.5 TeV. Outline of this model are as follows.

Initial distribution of nucleons inside a nucleus is taken from HIJING and is Woods-Saxon in nature. Scattering among them are treated with Eikonal formalism. If momentum transfer (Q^2) is greater than a cut off momentum (p_0), then these processes produce minijet partons and treated with PYTHIA model. Reverse ($Q^2 < p_0$) leads to production of strings. Depending on spin and flavor of excited strings, they get converted into partons without any further interaction. If those strings or partons satisfy minimum distance conditions ($\leq \sqrt{\sigma/\pi}$, σ being cross section for partonic two-body scattering), then they undergo interactions that are dealt by Zhang's Parton Cascade (ZPC) model [36]. Once these partons stop interacting, nearest two partons form a meson or that of three form a baryon using a quark coalescence model. Cascade of resultant hadrons is dealt by a relativistic transport model, ART [37, 38], which includes baryon-baryon, baryon-meson and meson-meson elastic and inelastic scatterings.

This version of AMPT, known as string melting has been used for the current study (version 26t5). There is another version referred as default AMPT model, where instead of quark coalescence, string fragmentation method is adopted.

2.3 The NLO model

The next-to-leading order, NLO-pQCD(MNR) [39] model used in the present work has been successfully used before to produce $c\bar{c}$ pair cross-sections in p+p collisions at most of the available collider energies [40]. Consequently the model can be used to produce various heavy quark spectra and can be utilised further to study various hot and dense nuclear matter effects (as in Pb+Pb and Au+Au collisions) and cold nuclear matter effects (as in p+Pb and d+Au collisions). In the present work, we have used the calculations to produce D-meson spectra for p+p collisions at $\sqrt{s} = 7$ TeV in order to check the consistencies of our calculations. In the next step, the calculations have been repeated for p+Pb at $\sqrt{s_{NN}} = 5.02$ TeV including shadowing effects as one of the initial cold nuclear effects [41, 42]. Let us now move to a brief description of the calculations:

The p_T differential spectrum of heavy quarks produced in p+p collisions is defined in general

as [40, 43]

$$E_1 E_2 \frac{d\sigma}{d^3p_1 d^3p_2} = \frac{d\sigma}{dy_1 dy_2 d^2p_{T_1} d^2p_{T_2}} \ , \tag{3}$$

where y_1 and y_2 are the rapidities of heavy quark and anti-quark and $p_{\mathbf{T}_i}$ are their transverse momenta.
In the above

$$\begin{aligned}\frac{d\sigma}{dy_1 dy_2 d^2p_{T_1} d^2p_{T_2}} = 2x_a x_b \sum_{ij} \Bigg[& f_i^{(a)}(x_a, Q^2) f_j^{(b)}(x_b, Q^2) \frac{d\hat{\sigma}_{ij}(\hat{s}, \hat{t}, \hat{u})}{d\hat{t}} \\ & + f_j^{(a)}(x_a, Q^2) f_i^{(b)}(x_b, Q^2) \frac{d\hat{\sigma}_{ij}(\hat{s}, \hat{u}, \hat{t})}{d\hat{t}} \Bigg] / (1 + \delta_{ij}) \ ,\end{aligned} \tag{4}$$

where x_a and x_b are the fractions of the momenta carried by the partons from their interacting parent hadrons.

We have used CTEQ6.6 structure function [44] as obtained using LHAPDF library for p+p system and added EPS09 [45] shadowing parameterization, to incorporate the initial nuclear effects on the parton densities for p+Pb system.

The differential cross-section for partonic interactions, $d\hat{\sigma}_{ij}/d\hat{t}$ is given by

$$\frac{d\hat{\sigma}_{ij}(\hat{s}, \hat{t}, \hat{u})}{d\hat{t}} = \frac{|M|^2}{16\pi \hat{s}^2}, \tag{5}$$

where $|M|^2$ (See Ref. 46) is the invariant amplitude for various partonic sub-processes both for leading order (LO) and next-to-leading order (NLO) processes as follows:
The physical sub-processes included for the leading order, $\mathcal{O}\ (\alpha_s^2)$ production of heavy quarks are

$$\begin{aligned} & g + g \to Q + \overline{Q} \text{ and} \\ & q + \bar{q} \to Q + \overline{Q} \ . \end{aligned} \tag{6}$$

At next-to-leading order, $\mathcal{O}\ (\alpha_s^3)$ subprocesses included are as follows

$$\begin{aligned} g + g &\to Q + \overline{Q} + g \ , \\ q + \bar{q} &\to Q + \overline{Q} + g \text{ and} \\ g + q(\bar{q}) &\to Q + \overline{Q} + q(\bar{q}). \end{aligned} \tag{7}$$

Next we discuss re-scattering processes within the nucleus. A parton may also undergo multiple hard scattering or a nucleon instead undergo multiple soft re-scattering within the cold nucleus in cases of p+A or A+A collisions. This is commonly referred as Cronin effects [20, 47]. These re-scatterings may lead to momentum broadening of the interacting partons and change the final heavy quark spectrum. This would also give rise to deviations of R_{pPb} from unity and is considered as another form of cold nuclear matter effect. We feel that its contribution apart from shadowing to the heavy meson spectra, when compared to p+p collisions, can be discerned with the precise state-of-the-art experiments designed at LHC-CERN and RHIC-BNL. However, it was earlier suggested that this effect may vanish at large transverse momentum region or high collider energies [48–50], but may be visible in the low and mid p_T region and is slowly emerging as a subject of contemporary interests in heavy ion collisions. The details of our implementations of the calculations are taken from Ref. 47, 51.

We can now discuss briefly about one of the mechanisms used from the above references. Starting with parton density functions, which can be defined as

$$f_i^{(a)}(x_a, Q^2, k_T^2) = f_i^{(a)}(x_a, Q^2).g_{p/A}(k_T^2) \ , \tag{8}$$

where $g_{p/A}(k_T^2) \propto \exp[-k_T^2/\pi . \langle k_T^2 \rangle_{pp/pA}]$ and $\langle k_T^2 \rangle_{pA} = \langle k_T^2 \rangle_{pp} + \langle k_T^2 \rangle_A$.

The effective transverse momentum kick, $\langle k_T^2 \rangle_{pA}$, following leads from Ref. 48 and 51, is obtained by adding $\langle k_T^2 \rangle_A$ as a consequence of series of re-scattering, to the intrinsic $\langle k_T^2 \rangle_{pp}$. Our preliminary assumption of taking this summation however doesn't extrapolate p + A system exactly to p + p scenario. We are currently looking to improve upon this assumption. The $\langle k_T^2 \rangle_A$ can be assumed as

$$\langle k_T^2 \rangle_A = \delta^2 . n . \ln \left(1 + \frac{p_T^2}{\delta^2 / c} \right) \tag{9}$$

where the parameters δ^2/c, average squared momentum kick per scattering and $n = L_A/\lambda\,, L_A = 4R_A/3$, average number of re-scattering, are used from Ref. 49, 51.

With the implementation of the above features, we can next fragment the charm momentum both from p+A and p+p collisions into D-mesons, as D-mesons data are readily verifiable from experiments. Schematically, this can be shown as

$$E\frac{d^3\sigma}{d^3p} = E_Q \frac{d^3\sigma}{d^3p_Q} \otimes D(Q \to H_M), \tag{10}$$

where the fragmentation of the heavy quark Q into the heavy-meson H_M is described by the function $D_D(z)$. We have assumed that distribution of D(z), w.r.t. z, where $z = p_D/p_c$, is used to calculate total D-mesons and is given by

$$D_D^{(c)}(z) = \frac{n_D}{z[1 - 1/z - \varepsilon_p/(1-z)]^2}, \tag{11}$$

where ε_p is the Peterson parameter $\simeq 0.12$ and is taken from Ref. 52. The normalization condition satisfied by the fragmentation function is

$$\int_0^1 dz\, D(z) = 1. \tag{12}$$

2.4 The FONLL model

As mentioned in the literatures, FONLL [53] has been used to calculate D-mesons spectra for LHC energies and earlier estimations have shown that FONLL calculation is able to explain various heavy quark observables particularly transverse momentum spectra of heavy mesons with remarkable accuracies. The p_T spectra of heavy quarks produced in p+p collisions as in Eq. 3 can be written as

$$E_c \frac{d\sigma}{d^3p_c dy_c} = \int d^3p_{\bar{c}} dy_{\bar{c}} \frac{d\sigma^{pp\to c\bar{c}}}{d^3p_c d^3p_{\bar{c}} dy_c dy_{\bar{c}}}\ , \tag{13}$$

where y_c and $y_{\bar{c}}$ are the rapidities of heavy quark and anti-quark and $p_{\mathbf{T}_i}$ are their transverse momenta.

The above distribution is evaluated at the Fixed-Order Next-to-Leading-Logarithmic (FONLL) level, implemented in Ref 53. In addition to the full fixed-order NLO result, the FONLL calculation also resums large perturbative terms proportional to $\alpha_s^n = \log^k(p_T/m_c)$ at all orders with next-to-leading-logarithmic (NLL) accuracy, where $m_c (= 1.5$ GeV) is the heavy quark mass. Here too, we have used CTEQ6.6 parton structure function and EPS09 shadowing parametrization for our calculations.

The charm fragmentation function developed by Cacciari *et al.* [54] is used in the present work. This depends on the parameter r (See Ref. 55) with the values of the parameters defined in the above references and fitted with e+e– spectra data. Bottom fragmentation instead depends on the parameter α_B in a functional form given by Kartvelishvili *et al.* [56] It is worth noting that using the Peterson *et al.* fragmentation function, gives a different result than that of fragmentation in FONLL [53].

3 Results and discussion

ALICE has recently published results on D-meson in p+p [57] and p+Pb [58] collisions. Keeping on view of that, events are generated at $\sqrt{s} = 7$ TeV and $\sqrt{s_{NN}} = 5.02$ TeV using all the above models, i.e. HIJING, AMPT, NLO and FONLL. For p+p system, the study is based on the mid rapidity region, i.e., $|y_{cms}| < 0.5$, where as for p+Pb system it is in the rapidity range -0.96 $< y_{cms} < 0.04$. We have ensured that no D-meson is coming from B-meson.

Normalised p+p yield was divided by $T_{pp} = 1.39 \times 10^{-5}$ μb^{-1} to obtain cross-section, while that for p+Pb T_{pPb} is 9.8334×10^{-5} μb^{-1} (calculated in Ref. 59).

From calculated cross-section, Nuclear modification factor (R_{pPb}) can be defined as follows:

$$R_{pPb} = \frac{(\frac{d\sigma}{dp_T})_{pPb}}{A \times (\frac{d\sigma}{dp_T})_{pp}}, \tag{14}$$

where A is the mass number of a nucleus (e.g., for Pb it is 208). Here we have used p+p collisions as baseline at $\sqrt{s_{NN}}$= 5.02 TeV. We will discuss these various cold nuclear matter effects on our results in the following sections.

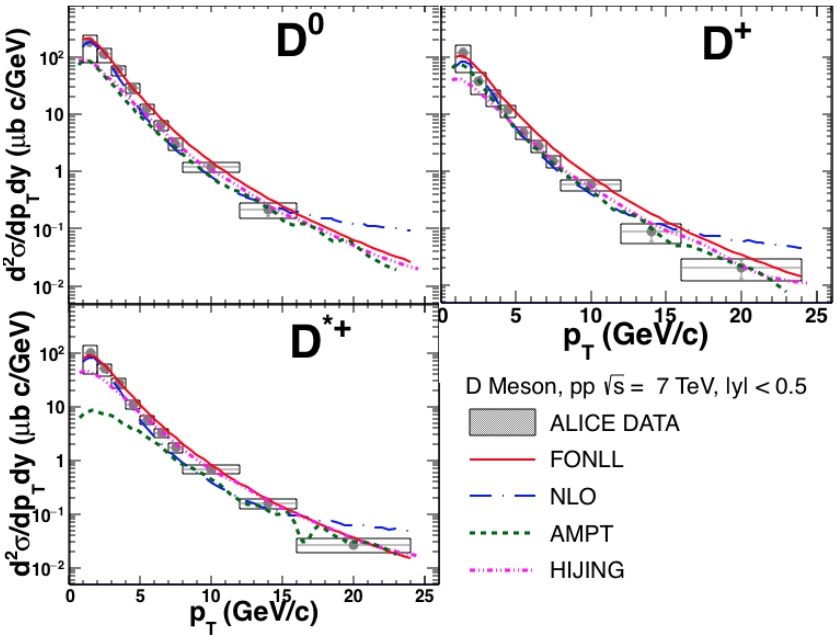

Figure 1: (Color online) p_T differential inclusive production cross-section of D-meson in p+p $\sqrt{s} = 7$ TeV. Solid markers represent the ALICE data points [57]. Statistical errors are in bars while systematic errors are in boxes. Small dash-dotted line (Magenta), dashed line (Green), long dash-dotted line (Blue) and solid line (Red) represent HIJING, AMPT, NLO and FONLL results, respectively.

Figure 1 shows transverse momentum (p_T) differential production cross-section of D^0, D^+ and D^{*+} mesons in p+p collisions at $\sqrt{s} = 7$ TeV. Except for few low p_T bin, HIJING explains data within the uncertainties. Similar trend is followed by AMPT for D^0 and D^+, but it poorly explains cross section of D^{*+} for $p_T < 10$ GeV/c. Apart from the direct production of D^0 and D^+, we have incorporated contributions from other resonance decays. However, there is no decay contribution of other particles for the production of D^{*+}. From figure 1, we may say that both String Fragmentation and quark coalescence based simulation models (HIJING and AMPT respectively) are able to explain results from p+p collision data. In addition to that, there might be some additional production mechanism is needed for AMPT especially at low p_T, which might add up to the D^{*+} cross-section. NLO results explains the data within error bars

up to $p_T < 15$ GeV/c, but over estimates the results at higher p_T region. This may be due to the large NLO contributions adopted in the model formalism. Its shape is different from other simulations, which might be due to its dependence on renormalisation and fragmentation scale factors. FONLL at its next-to-leading calculations explains data very well for all p_T region.

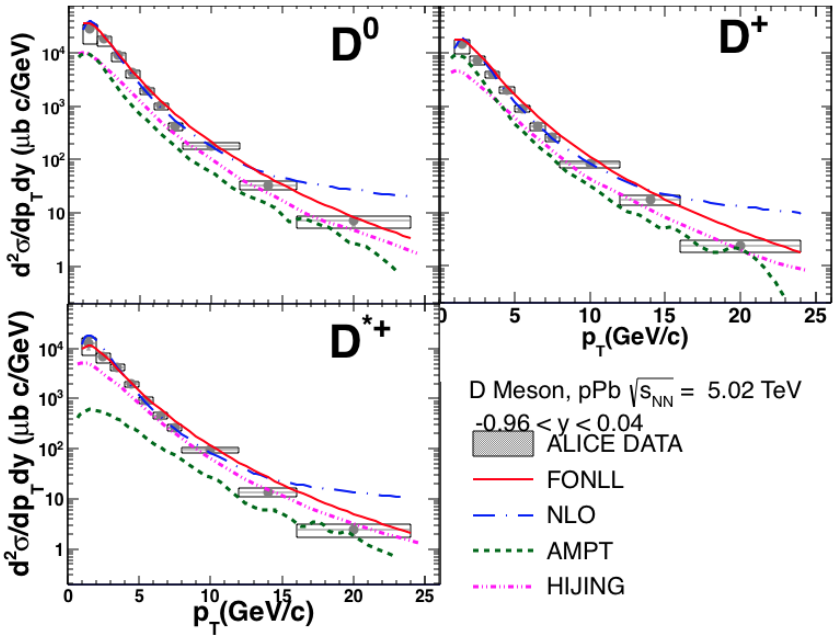

Figure 2: (Color online) p_T differential inclusive production cross-section of D-meson in p+Pb data at $\sqrt{s_{NN}} = 5.02$ TeV. Solid markers represent the ALICE data points [58]. Statistical errors are in bars while systematic errors are in boxes. Small dash-dotted line (Magenta), dashed line (Green), long dash-dotted line (Blue) and solid line (Red) represent HIJING, AMPT, NLO and FONLL results, respectively.

Figure 2 is same as that of Figure 1, but for p+Pb system at $\sqrt{s_{NN}}$= 5.02 TeV. Here HIJING under-predicts the data for $p_T < 7$ GeV/c. So we may think that cold nuclear shadowing effect of Pb as implemented in this model might have suppressed the yield to a large extent. AMPT under-predicts the data for all p_T region for D^0 and D^+, but have same miss-match as that of p+p for the case of D^{*0}. On contrary to HIJING, AMPT shows a smaller production cross-section for D^0 and D^+ in p+Pb system in its mechanism irrespective of nuclear shadowing effect. NLO in p+Pb likewise over estimates the cross-section for $p_T > 15$ GeV/c. FONLL explains data for all p_T to very good extent.

Figure 3 shows p_T-dependence of average R_{pPb} of D^0, D^+ and D^{*+} mesons in p+Pb data at $\sqrt{s_{NN}} = 5.02$ TeV. The calculations from HIJING and AMPT are showing prominent cold nuclear matter (CNM) effects such as shadowing, EMC [60], and multi-parton scattering effects, for the entire p_T range. The results under-estimate the magnitude and trend of experimental data. The reasons behind such large CNM effects implemented in these calculations are being investigated and will be reported in our future publications. Besides having quark coalescence as parton production mechanisms in AMPT than that of string fragmentation in HIJING, AMPT has additional partonic and hadronic transport parts which have both elastic and inelastic scatterings. This may also be the reason that R_{pPb} from AMPT is lower than that of HIJING. Next, in case of NLO, which has its nuclear shadowing feature, and in addition, it has momentum broadening effect (Cronin) due to re-scattering. Both the results with and without the momentum broadening effects are shown in the plot. The corresponding result with additional momentum broadening are closer to the trend of the data within its error bars. The result using NLO without broadening is closer to unity with suppression at the low p_T region due to shad-

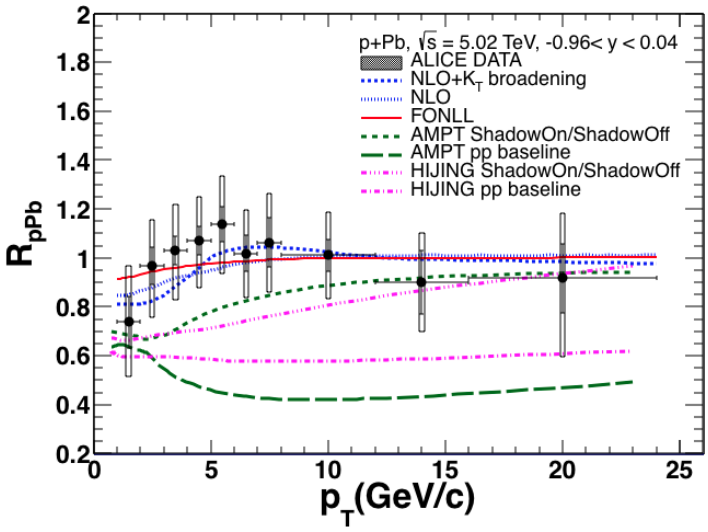

Figure 3: (Color online) Nuclear modification factor for D-meson in p+Pb at $\sqrt{s_{NN}}$= 5.02 TeV. Solid markers represent the ALICE data points [58]. Statistical errors are in bars while systematic errors are in boxes. Dash-dotted line (Magenta), dashed line (Green), solid line (Red) and dotted line (Blue) represent HIJING, AMPT, FONLL and NLO results respectively. AMPT ShadowOn/ShadowOff or HIJING ShadowOn/ShadowOff represent results from taking nuclear effect shadowing on in numerator to off in denominator (other nuclear effects kept un-changed) in the same system , i.e. p+Pb at $\sqrt{s_{NN}}$= 5.02 TeV.

owing and shows a difference in the shape of the curve from the one including the broadening effect. We may recall that a similar enhancement in trend of R_{dAu} for π_0 meson has also been reported for d+Au collisions at $\sqrt{s_{NN}}$ = 5.5 TeV by M. Gyulassy *et al.* (see Ref. 51). FONLL with shadowing features only too gives very small shadowing effect for $p_T < 10$ GeV/c and remains close to unity.

Using AMPT and HIJING, to show the effects of shadowing exclusively on nuclear modification factor and also difference between p + p and p+Pb (shadow-off) as baselines, we further calculated R_{pPb} as following:

$$R_{pPb} = \frac{(\frac{d\sigma}{dp_T})^{ShadowOn}_{pPb}}{(\frac{d\sigma}{dp_T})^{ShadowOff}_{pPb}} \quad (15)$$

Here we have turned on shadowing effect in numerator and turned it off in denominator (while other nuclear effects like multi-parton scattering etc. are present in both) in the same system, i.e. p+Pb at $\sqrt{s_{NN}}$= 5.02 TeV. As we can see from Figure 3 that taking p+Pb (shadow-off) as the baseline we see considerable nuclear effects such as shadowing particularly at the low and intermediate p_T regions, while any other effects due to Pb nucleus is cancelled both from numerator and denominator of the ratio. The results however differ much from calculations using p + p baseline (AMPT and HIJING), suggesting greater effects of multi-parton scattering than shadowing etc. on the final D meson spectra.

4 Summary

We have carried out D-meson study in simulation models like HIJING and AMPT and compared our results with published ALICE data for p+p collisions at $\sqrt{s}$ = 7 TeV and p+Pb collisions at $\sqrt{s_{NN}}$ = 5.02 TeV. We have also compared with the results from next-to-leading order calculations from FONLL and NLO.

Irrespective of shadowing effect included in both the models, AMPT shows lower value of R_{pPb} compared to HIJING above $p_T = 2.5$ GeV/c. So we may conclude that magnitude of R_{pPb} in AMPT due to its additional partonic and hadronic transport parts differs from the same in HIJING. And for resonance particle D^{*+}, additional mechanism is needed in AMPT to explain its production cross-section. More details in this direction will be reported in our future study.

Since R_{pPb} in all our calculations deviates from unity, thus there is initial cold nuclear matter effect playing an important role in all models. K_T broadening can predict the shape of the data. Also taking p+Pb (shadow off) as baseline in AMPT and HIJING highlights shadowing effect exclusively, other nuclear effects like multi-parton scattering phenomenon has considerable effects and can be viewed only with p + p as baseline. To end with, further improvements are required in our parameter dependent models, to explain the experimental data properly. If results from high statistics data with improved uncertainty be available in future, we will improve these parameter dependent models to fit with data.

References

[1] https://www.bnl.gov/rhic/

[2] http://home.cern/topics/large-hadron-collider

[3] J. C. Collins and M. J. Perry, Phys. Rev. Lett. **34**, 1353 (1975); L. D. McLerran and B. Svetitsky, Phys. Lett. **B 98**, 195 (1981).

[4] K. Kajantie, C. Montonen and C. Pietarinen, Zeit. Phys. **C 9**, 253 (1981); R. Hagedorn and J. Rafelski, Phys. Lett. **B 97**, 180 (1980).

[5] J. W. Harris and B. Müller, Ann. Rev. Nucl. Part. Sci. **41**, 96 (1996); B. Müller, Rep. Prog. Phys. **58**, 611 (1998).

[6] S. A. Bass, M. Gyulassy, H. Stöcker and W. Greiner, J. Phys. **G**: Nucl. Part. Phys. **25**, R1-R57 (1999).

[7] http://www.star.bnl.gov/

[8] J. Adams et al. (STAR Collaboration) Nucl. Phys. A 757 (2005) 102-183

[9] http://home.cern/about/experiments/alice

[10] B. Abelev et al. (ALICE Collaboration) Int. J. Mod. Phys. A Vol. 29 (2014) 1430044

[11] http://www.fair-center.eu/for-users/experiments/cbm.html

[12] B. Friman et al. (Compressed Baryonic Matter in Laboratory Experiments) Lecture Notes in Physics, Vol. 814 (Springer, 2011)

[13] Guang-You Qin and Xin-Nian Wang, *Int. J. Mod. Phys. E* **24**, 1530014 (2015)

[14] A. Drees, Nucl. Phys. **A 698**, 331 (2002); E. Shuryak, Nucl. Phys. **A 750**, 64 (2005); S. Jeon and G. D. Moore, Phys. Rev. **C 71**, 034901 (2005).

[15] X-N. Wang, Nucl. Phys. **A 750**, 98 (2005); A. K. Chaudhuri, Phys. Lett. **B 659**, 531 (2008); David d'Enterria and B. Betz, Lect. Notes Phys. **785**, 285 (2010).

[16] A. Adare *et al.* (PHENIX Collaboration), Phys. Rev. Lett. **98**, 172301 (2007); B. I. Abelev *et al.* Phys. Rev. Lett. **98**, 192301 (2007);

[17] S. K. Das, F. Scardina, S. Plumari and V. Greco, Phys. Lett. **B 747**, 260 (2015); S. K. Das, J. e. Alam and P. Mohanty, Phys. Rev. **C 82**, 014908 (2010).

B. Abelev *et al*, (ALICE Collaboration), arXiv:1203.2160v1[nucl-ex]2012.

[18] M G Wysocki (PHENIX collaboration), Nucl. Phys. A **904-905**, 67c-74c (2013) M Sarsaur (PHENIX collaboration), Nucl. Phys. Proc. **276-278**, 125-128 (2016).

[19] K. J. Eskola, V. J. Kolhinen and C. A. Salgado, Eur. Phys. J. **C 9**, 61 (1999); K. J. Eskola, V. J. Kolhinen, P. V. Ruuskanen and C. A. Salgado, Nucl. Phys. **C 661**, 645 (1999).

[20] J. W. Cronin, H. J. Frisch, M. J. Shochet, J. P. Boymond, R. Mermod, P. A. Piroue and R. L. Sumner, Phys. Rev. **D 11**, 3105 (1975).

[21] A. Adare *et al.* (PHENIX Collaboration), Phys. Rev. Lett. **98**, 172301 (2007).

[22] E. Eichten, I. Hinchliffe, K. D. Lane, and C. Quigg, Rev. Mod. Phys. **56**, 579 (1984); Z. W. Lin, and M. Gyulassy,Phys. Rev. **C 51**, 2177 (1995); M. Younus and D. K. Srivastava, J. Phys. G: Nucl. Part. Phys. **37**, 115006 (2010).

[23] A. Adare *et al*, (PHENIX Collabodation), Phys. Rev. Lett. **109**, 242301 (2012); G. Luparello, for the ALICE Collaboration, Journal of Physics: Conference Series, **509**, 012101 (2014); C. Jena, for the ALICE Collaboration, Journal of Physics: Conference Series, **535**, 012027 (2014).

[24] H. Fujii and K. Watanabe, arXiv:1308.1258, (2013).

[25] X N Wang, M Gyulassy, Phys. Rev. **D 44**, 3501 (1991).

[26] B. Andersson, G. Gustafson, and B. Nilsson-Almqvist, Nucl. Phys. **B 281**, 289 (1987); B. Nilsson-Almqvist and E. Stenlund, Comp. Phys. Commun. **43**, 387 (1987).

[27] A. Capella, U. Sukhatme, and J. Tran Thanh Van, Z. Phys. **C 3**, 329 (1980); J. Ranft, Phys. Rev. **D 37**, 1842 (1988); J. Ranft. Phys. Lett. **B 188**, 379 (1987).

[28] T. Sjostrand and M. van Zijl, Phys. Rev. **D 36**, 2019 (1987); T. Sjostrand, Comput. Phys. Commun.**39**, 347 (1986); T. Sjostrand and M. Bengtsson, ibid. **43**, 367 (1987).

[29] C. W. Dejager, H. DeVries, and C. DeVries, At. Data Nucl. Data Tables **14**, 479 (1974).

[30] M. Gyulassy, in Proceedings of Eighth Balaton Conference on nuclear Physics, edited by Z. Fodor (KFKI, Budapest, 1987); CERN Report No. CERN-TH-4794/87, 1987.

[31] E. Eichten, I. Hinchliffe, K. Lane, and C. Quigg, Rev. Mod. Phys. **56**, 579 (1984).

[32] D. W. Duke and J. F. Owens, Phys. Rev. **D 30**, 50 (1984).

[33] A. H. Mueller and J. Qiu, Nucl. Phys. **B 268**, 427 (1986); J. Qiu, ibid. **B 291**, 746 (1987).

[34] L. L. Frankfurt and M. I. Strikman, Phys. Rep. **160**, 235 (1988).

[35] Zi-Wei Lin, Che Ming Ko, Bao-An Li and Bin Zhang, Subrata Pal Phys. Rev. C **72**, 064901 (2005).

[36] B. Zhang, Comput. Phys. Commun. **109**, 193 (1998).

[37] B. A. Li, A. T. Sustich, B. Zhang and C. M. Ko, Int. J. Mod. Phys. **E 10**, 267 (2001).

[38] B. A. Li and C. M. Ko, Phys. Rev. **C 52**, 2037 (1995).

[39] M. L. Mangano, P. Nason and G. Ridolfi, Nucl. Phys. **B 373**, 295 (1992); S. Frixione, M. L. Mangano, P. Nason and G. Ridolfi, Adv. Ser. Direct. High Energy Phys. **15**, 609 (1998).

[40] U. Jamil and D. K. Srivastava, J. Phys. **G 37**, 085106 (2010).

[41] K. J. Eskola, H. Honkanen, V. J. Kolhinen and C. A. Salgado, hep-ph/0302170 (1999); J. QIU, Nucl. Phys. **B 291**, 746 (1987).

[42] R. Vogt, arXiv:1508.01286 [hep-ph].

[43] M. Younus, U. Jamil and D. K. Srivastava, J. Phys. **G 39**, 025001 (2012).

[44] P. M. Nadolsky, H.-L. Lai, Q.-H. Cao, J. Huston, J. Pumplin, D. Stump, W.-Ki. Tung, C.-P. Yuan, Phys. Rev. **D 78**, 013004 (2008).

[45] K. J. Eskola, H. Paukkunen and C. A. Salgado, JHEP **0904**, 065 (2009).

[46] B. L. Combridge Nucl. Phys. B **151**, 429 (1979).

[47] A. Accardi, hep-ph/0212148 (2003); X.-N. Wang, Phys. Rev. **C 61**, 064910 (2000).

[48] A. Accardi, M. Gyulassy, Phys. Lett. **B 586**, 244 (2004).

[49] R. Sharma, I. Vitev, and B.-W. Zhang, Phys. Rev. **C 80**, 054902 (2009).

[50] G. G. Barnafoldi, P. Levai, G. Fai, G. Papp and B. A. Cole, Int. J. Mod. Phys. **E 16**, 1923 (2007)

[51] I. Vitev, and M. Gyulassy, Phys. Rev. Lett. 89, No. 25, 252301 (2002); I. Vitev, Phys. Lett. **B 562**, 36 (2003).

[52] C. Peterson, D. Schlatter, I. Schmitt, and P. Zerwas, Phys. Rev. **D 27**, 105 (1983).

[53] M. Cacciari, M. Greco and P. Nason, JHEP **9805**, 007 (1998); M. Cacciari, PoS HEP **2005**, 137 (2006) [arXiv:hep-ph/0512251].

[54] M. Cacciari and P. Nason, JHEP **0309**, 006 (2003).

[55] E. Braaten, K. Cheung, S. Fleming, and T. C. Yuan, Phys. Rev. **D 51**, 4819 (1995) [arXiv:hep-ph/9409316].

[56] V. G. Kartvelishvili, A. K. Likhoded, and V. A. Petrov, Phys. Lett. **B 78**, 615 (1978).

[57] B. Abelev *et al.* (ALICE Collaboration), JHEP 01 **128** (2012).

[58] B. Abelev *et al.* (ALICE Collaboration), Phys. Rev. Lett. **113**, 232301 (2014)

[59] M. Mangano, H. Satz and U. Wiedermann, DOI 10.5170/CERN-2004-009, http://cds.cern.ch/record/815037; J. Adam *et al.* (ALICE Collaboration), Phys. Rev. **C 91**, 064905 (2015)

[60] EM Collab., J. Ashman, et al., Phys. Lett. 202B, 603 (1988); EM Collab., M. Arneodo, et al., Phys. Lett. 211B, 493 (1988).